Coline MAUREL

GEN
2022-2023

Okayama University
1 Chome-1-1 Tsushimanaka, Kita Ward, Okayama, 700-8530, Japan

Estimation of pointing systematics offset for Cosmic Microwave Background polarization analysis

du 07/05/2023 au 11/08/2023

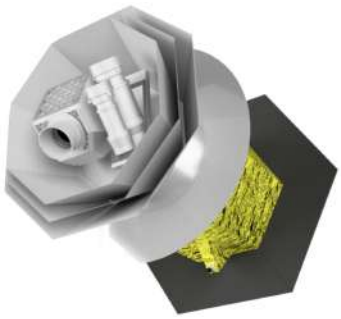

Under the supervision of:

1. **Internship Supervisor**: Hirokazu ISHINO
   email: scishino_at_s.okayama-u.ac.jp
2. **School Supervisor**: Nicolas CAPELLAN
   email: nicolas.capellan@grenoble-inp.fr

Ecole nationale
supérieure de physique,
électronique, matériaux

Phelma
Bât. Grenoble INP - Minatec
3 Parvis Louis Néel - CS 50257
F-38016 Grenoble Cedex 01

Tél +33 (0)4 56 52 91 00
Fax +33 (0)4 56 52 91 03

Confidential: No

Acknowledgements

I would like to thank my supervisor Professor Hirokazu Ishino for giving me the opportunity to work in his laboratory. This internship has been very enriching for me. I discovered the world of research in an international context in a field I had never studied before. Therefore, this experience has significantly improved my adaptability skills. Secondly, I am glad to had the chance to live in Japan because it is a wonderful country. I strongly appreciate traveling around Japan but what I prefer the most is the Japanese people kindness.

I would also like to thank sincerely Yusuke Takase, a PhD student from the laboratory. Yusuke helped me a lot during my internship. He shared to me his knowledge and his experience in cosmology. Thanks to him, I could progress with confidence in my work. He is also behind a number of tools that I used to get my results.

I am also thankful to Mr Bernard Chenevier and Ms Valery Parry for being the coordinators of my internship. They allowed me to apply for this internship and then took care of getting me in touch with Pr. Hirokazu Ishino. This experience would have never happened without them.

Finally, I would like to express my gratitude to all the students of the laboratory, especially Raffuzzi Nicolò, Bortolami Marco, Nagano Yuya and Morinaga Mami, for their help. I have learned about cosmology in a wonderful working environment thanks to them.

Contents

Glossary **2**

List of figures **2**

List of tables **2**

Introduction **2**

1 Introduction to Cosmology **6**
1.1 Observation of the universe . . . 6
1.2 Cosmic Microwave Background (CMB) . . . 6
1.3 Cosmic Inflation and LiteBIRD satellite . . . 6

2 CMB anisotropies **8**
2.1 Temperature and Polarization anisotropies . . . 8
2.2 Representation of CMB maps and power spectrum: Healpix . . . 10

3 LiteBIRD systematics **12**
3.1 LiteBIRD systematics errors . . . 12
3.2 Introduction to pointing systematics . . . 14
3.3 Reconstructed maps including pointing errors . . . 15

4 Foregrounds **17**
4.1 Introduction to Foregrounds . . . 17
4.2 Preparation of Foregrounds and Component separation . . . 17

5 Estimation of Δr **19**
5.1 Resolution scheme . . . 19
5.1.1 Generation of Foregrounds and CMB maps . . . 19
5.1.2 Reconstruction of maps with pointing offsets . . . 20
5.1.3 Deconvolution . . . 20
5.1.4 Component separation and calculation of the residual CMB . . . 20
5.1.5 Mask operation . . . 21
5.2 Outcomes . . . 22
5.2.1 Power spectrum . . . 22
5.2.2 Δr as a function of the pointing systematic offset . . . 23
5.2.3 Comparison to another resolution method . . . 24

Conclusion **24**

References **24**

Résumé **24**

Abstract **24**

Glossary

CMB: Cosmic Microwave Background

JAXA: Japan Aerospace Exploration Agency

NASA: National Aeronautics and Space Administration

ESA: European Space Agency

COBE: The Cosmic Background Explorer

WMAP: Wilikinson Microwave Anisotropy Probe

LiteBIRD: The Lite (Light) satellite for the study of B-mode polarization and Inflation from cosmic background Radiation Detection

LFT: Low Frequency Telescope

MFT: Medium Frequency Telescope

HFT: High Frequency Telescope

TOD: Time Ordered Data

PYTHON: programming language used for many applications such as cosmology

JULIA: programming language for computational science

FALCONS: Framework for Astrophysical Locus Computing ON the Sky

Psym3: Library used to create realistic maps of the sky at different frequency and different angular resolution

FGBuster: ForeGroundBuster library which provides easy-to-use functions to perform component separation of sky maps into different frequency maps

FWHM: Full Width at Half Maximum

List of Figures

1 Horizon problem . . . 7
2 Flatness problem . . . 7
3 Angular Scale Fluctuations . . . 8
4 CMB map and Temperature power spectrum from Planck mission . . . 8
5 Thomson scattering of quadrupole anisotropies create linear polarization . . . 9
6 Representation of E and B mode . . . 9
7 Ring Order, visualization of the scheme for nside=2, nside=4, nside=8, nside=16 . . . 10
8 CMB anistropies . . . 10
9 CMB power spectrum . . . 11
10 Decomposition of δr between margins, statistics and systematics . . . 12
11 Smoothing operation . . . 13
12 Power spectrum for the smoothing operation . . . 13
13 Low, Mid and High-Frequency Telescopes (left) and LFT detectors configuration (right) 14
14 LiteBIRD telescopes . . . 14
15 Pointing systematic error . . . 15
16 LiteBIRD scanning strategy . . . 16
17 LiteBIRD scanning path for 5000s, 1 day, 1month and 1 year . . . 16
18 Reconstructed map program results with 1 arcmin offset (temperature) . . . 16
19 Distribution of Foregrounds across the frequency . . . 17
20 Foregrounds at the frequency $f = 78.0GHz$ . . . 18
21 Foregrounds and CMB at the frequency $f = 78.0GHz$ . . . 18
22 Component separation result. Residual between the input CMB and CMB after the component separation . . . 18
23 Resolution scheme for the estimation of δr . . . 19
24 Creation of CMB maps with Foregrounds (dust and synchrotron), smoothed according to the 22 LiteBIRD beam size . . . 20
25 Pointing systematics scan : 0 arcmin offset, 1 arcmin offset, no arcmin offset . . . 20
26 Temperature maps before and after the deconvolution operation . . . 21
27 Residual CMB = $CMB_{0arcmin} - CMB_{1arcmin}$ . . . 21
28 Galactic plane mask with 0 (left) and 2 degrees apodization (right) . . . 21
29 Residual CMB, Temperature and Polarization anistropies with the galactic plane mask . 22
30 Residual CMB power spectrum (with or without galactic plane mask) . . . 22
31 Residual CMB power spectrum for several pointing offsets) . . . 23

List of Tables

1 LiteBIRD frequency bands and beam sizes . . . 14

Introduction

The aim of Cosmology is to observe and explain the universe we live in. Currently, the model that best describes the evolution of the universe is the "Big Bang". It proposes that the universe is expanding from an initial hot and dense state. This theory helps explain several phenomena that we observe such as the presence of the Cosmic Microwave Background (CMB), a microwave radiation that fills all the space around us. In the late 1970s, physicists such as Alexei Alexandrovich Starobinsky introduced the theory of Cosmic Inflation to complete the Big Bang model. It suggests an exponential expansion of the early universe. This theory could solve many unsolved problems such as the extreme uniformity of the universe, known as the horizon problem. In fact, the universe could have been homogenized before this inflationary period.

However, the theory of Cosmic Inflation still needs to be proven, and the CMB provides a unique way to do it. In fact, if we had to summarize the progress of research to prove cosmic inflation, we would have said that we still have to calculate a parameter, noted r, hidden in this micrometric radiation. More precisely, to calculate "r", we need to study the polarization anisotropies of the CMB. That is why, the JAXA (Japan Aerospace Exploration Agency) created the LiteBIRD project which aims to launch an international satellite around 2030 to study the polarization anisotropies of the CMB.

The satellite will have to meet many specifications to minimize the error made in the calculation of "r". Some errors called "systematics" are often made by the instrument and should be controlled early before launch. For example, pointing systematics errors occurs when we believe we are pointing in a certain point in space when in fact, we are slightly off-target. Pointing errors could totally bias the estimates on r. In this report, we will ask how much pointing error is acceptable to obtain a sufficient estimation on r, to validate or not the theory of cosmic inflation.

Therefore, the objective of my work is to define a specification for the acceptable range of pointing error for the LiteBIRD instrument. This specification is essential to construct the satellite, without which we will not be able to validate the cosmic inflation theory. This report will cover several cosmological parameters and it will present the results I obtained through simulations which I obtained with two different programming languages, Julia and Python.

This report contains five sections. The first one will present the essential cosmological insights to understand the content of my work. Then, I will focus on CMB anisotropies and more specifically, I will depict the different types of polarization. Afterwards, I will define systematic errors and present the LiteBIRD satellite. Subsequently, I will talk about foregrounds, one of the most important perturbations to study the CMB polarization and finally, I will present my resolution scheme and my results for estimating the pointing systematic offset.

1 Introduction to Cosmology

1.1 Observation of the universe

Cosmology is a scientific discipline whose aims to study the Universe. Usually, it deals with large objects so that the SI units are not really convenient [1]. For instance, instead of using meters, we would prefer to use system solar distances such as astronomical unit AU (distance between Earth and Sun), interstellar distances like the parsec pc (distance between Earth and Proxima Centauri, the nearest star of the Sun) or intergalactic distances as Megaparsec Mpc (distance between us and M31, the Andromeda galaxy). We also use the mass of the Sun M0 as the unit for mass and the Gyr as the unit for time (The age of the Earth is 4.6 Gyr).

The study of the universe began with observations. One of the main observations we have made is certainly the redshift of galaxies which is a very important clue to prove the expansion of the universe. The Big Bang model is an obvious phenomenon which comes the expansion of the universe : "it expands from an initially highly dense and hot state to its current low density state" [1]. In the middle of the 20th century, another cosmological model was considered : the Steady State Model. It provides that there are "no privileged locations in space or privileged moments in time" [1] . However, recent observations and especially the Cosmic Microwave Background (CMB) discovery, have led many scientists to reject the Steady State Model.

1.2 Cosmic Microwave Background (CMB)

If the universe was as hot as the Big Bang model suggests, the baryonic matter (made up of protons and neutrons) was ionized so that the numerous free electrons created by ionizations made the universe opaque. Therefore, the primordial plasma emitted blackbody radiation. However, as the universe expanded, the universe cooled. And, when its temperature dropped to 3000 K, electrons and protons could come together to create atoms. This phase is called the "recombination". As photons can pass through atoms, when we dropped to 3000 K, the universe was no longer opaque but transparent.

For many scientists at the time, if the Big Bang model was true, there had to be a relic of the radiation of the Blackbody at 3000 K. It was only in 1964, that two radio-astronomers, Arno Penzias and Robert Wilson, pointed out the background radiation without knowing what they were doing. The radiation they detected was close to 3K instead of 3000K because of the expansion of the universe: the expansion tends to stretch the wavelengths. Hence, the current temperature of the CMB is equivalent to a microwave radiation :

$$T = 2,25 \pm 5\,\mathrm{K} \tag{1}$$

Numerous projects have been led since this major breakthrough. For instance, NASA launched COBE (The Cosmic Background Explorer) in 1989 which yielded important insights about the radiation. For instance, it has shown that the CMB is well fitted by a blackbody spectrum, which is in line with its presumed origin. COBE observations also revealed CMB temperature anisotropies that permit us to know, among other things, the composition and the age of the universe. And last but not least, the CMB presents polarization anisotropies made by Compton scattering. The study of these latter anisotropies could help us to understand what happened at the beginning of the universe -for instance, validating of not theories such as Cosmic Inflation.

1.3 Cosmic Inflation and LiteBIRD satellite

The theory of Cosmic Inflation was introduced in the late 1970s. It permits to solve many issues that the Big Bang theory alone cannot address, although it still requires to be demonstrated. The Cosmic Inflation theory suggests that the Big Bang includes a period of exponential expansion of the Universe. In fact, it attempted that the size of the universe increased by a factor of 10^{30} during 10^{-30} seconds. This inflation would have created primordial fluctuations, the origin of the CMB anisotropies. Inflation is really convenient because it permits us to solve two main issues that cosmologists used to deal with.

The first one is called "the horizon problem". Distant regions of space are so far away that, according to the expansion of the universe, they have never been able to be in contact. Nevertheless, these regions have similar properties. For instance, the temperature of the CMB is approximately the same in every direction. How to explain this homogeneity if these regions have never seen each other?

This is the horizon problem. Inflation could solve it because it suggests that the universe had time to homogenize before it exploded.

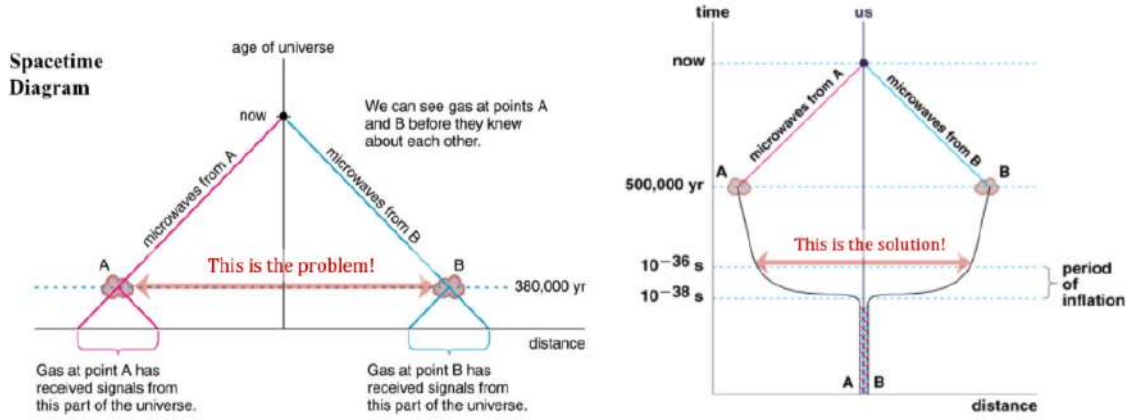

Figure 1: Horizon problem

The second issue that inflation could solve is "the flatness problem". In fact, every previous calculation has shown that the Universe has zero curvature which means that it is flat. These results imply that the density of the universe must have a really specific value. Since we do not believe in coincidence, there has to be a particular reason to explain why the universe is so flat [2]. Inflation can be the one. Actually, if the universe exponentially expanded during a very short time, it would have flattened the universe.

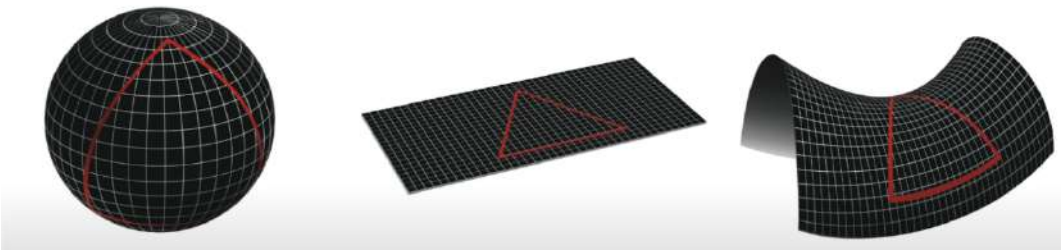

Figure 2: Flatness problem

Therefore, Cosmic Inflation offers many explanations of the evolution of the universe that cannot be resolved by the Big Bang theory alone. However, it still has to be proved. That is why the LiteBIRD project was initiated by JAXA (Japan Aerospace Exploration Agency). This project aims to launch an international satellite around 2030, to search for evidence of Cosmic Inflation by studying CMB polarization. In fact, inflation theory suggests that the primordial gravitational waves [1] created during inflation would have imprinted a specific pattern in CMB polarization called "B-mode". Besides, the study of this pattern could raise valuable evidence that supports the occurrence of Cosmic Inflation during the first time of the universe.

[1] Deformation waves of space-time that are usually very weak. To detect them, we need very massive objects undergoing a strong acceleration, such as the Inflation period

2 CMB anisotropies

2.1 Temperature and Polarization anisotropies

The temperature of the CMB is extremely uniform across the sky with an average temperature of 2.7 Kelvin. However, it presents tiny fluctuations around a hundred microkelvins. To represent these fluctuations over the sky we use a tool called the "power spectrum" which allows the decomposition of temperature fluctuations into different angular scales. To understand what is an angular scale, we present the figure 3 extracted from [2]. In this figure, we have sinusoidal fluctuations at two different angular scales : at 5 and 60 degrees.

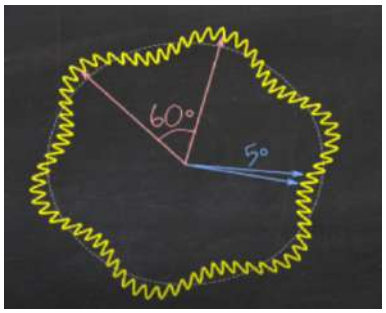

Figure 3: Angular Scale Fluctuations

To obtain the power spectrum, we describe temperature data with spherical harmonics which are mathematical functions used to describe variations on a sphere. Spherical harmonics are characterized by two parameters : m and l. For example, if we consider a random vector on the sphere, denoted as $\mathbf{n}$, the variation of temperature at a specific point defined by $\mathbf{n}$ can be expressed as :

$$\Delta T(\mathbf{n}) = \sum_{l,m} a_{lm}^T Y_{lm}(\mathbf{n}) \tag{2}$$

Where Y_{lm} are spherical harmonics and a_{lm} is a coefficient which characterizes the intensity of the fluctuation. The power spectrum is given by :

$$C_l = \frac{1}{2l+1} \sum_m a_{lm} a_{lm}^* \tag{3}$$

By applying this decomposition, we get access to large scale fluctuations (corresponding to low value of l) and finer details (high value of l) of temperature fluctuations.

In 2009, the European Space Agency (ESA), with the collaboration of NASA, launched "Planck", a satellite conceived to measure CMB temperature anisotropies with much higher sensitivity than its predecessors COBE and WMAP. Figure 4 gives Planck results, the most precise results we have currently. In particular, this power spectrum provided many information about the universe, such as its composition or its age.

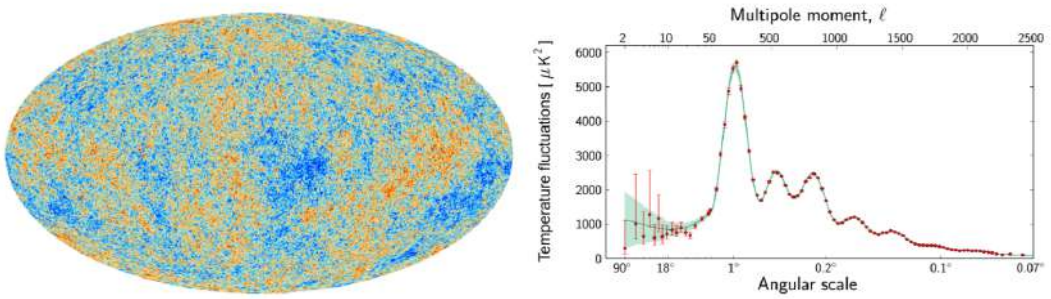

Figure 4: CMB map and Temperature power spectrum from Planck mission

So far, the focus of CMB studies has been on temperature anisotropies. The next challenge is to measure CMB polarization which would also provide additional information about our universe. For instance, the polarization of the CMB provides a way to study the gravitational waves produced during Inflation. When light is polarized, the electric field oscillates in a particular direction, perpendicular to the direction of propagation. Therefore, polarization provides numerous information about the electromagnetic wave we are studying, but light is not necessarily polarized. By chance, CMB is polarized due to Thomson scattering (figure 5, an elastic scattering of electromagnetic waves by free-charge particles. In the CMB case, photons were constantly scattered by electrons until the recombination phase where photons were no longer trapped and were free to spread throughout the universe. So, the CMB polarization we see now is the last scattering of photons by electrons during the recombination.

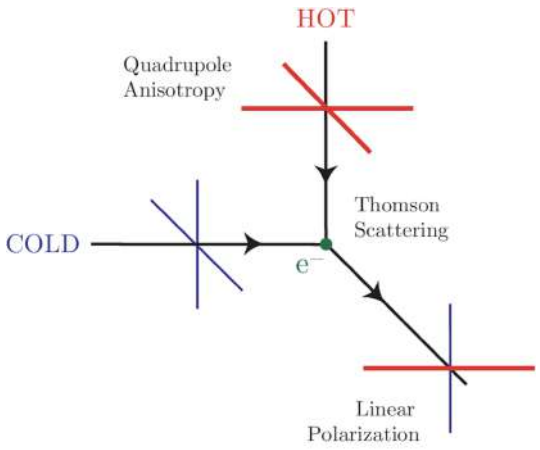

Figure 5: Thomson scattering of quadrupole anisotropies create linear polarization

To describe the distribution of radiation polarization on the celestial sphere, we use the Stokes parameters Q and U defined as:

$$\begin{cases} Q = E_x^2 - E_y^2 \\ U = E_a^2 - E_b^2 \end{cases} \tag{4}$$

Where E_a is the 45-degree direction in the x-y plane and E_b the perpendicular direction. Of course, Q and U depend on the way we choose the coordinate system but for the CMB analysis, we prefer to use variables that are independent of the rotation. Hence, we use two quantities [2] called "E-mode" and "B-mode"[3] as shown in figure 6.

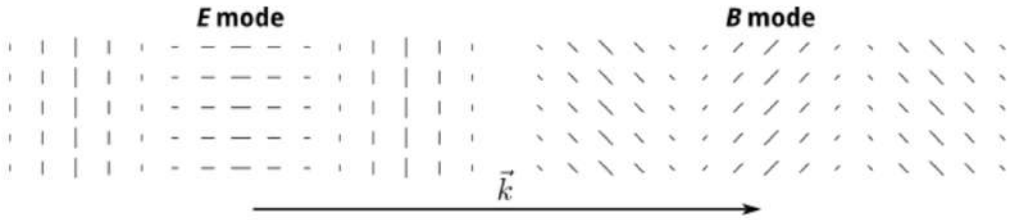

Figure 6: Representation of E and B mode

The main contribution to the CMB polarization is density perturbations but these have only created E-mode patterns whereas gravitational waves from inflation have both printed E-mode and B-mode polarization. That is why, LiteBIRD aims to detect the B-mode polarization, which has never been clearly detected before because it remains difficult. In fact, E-mode amplitude is larger than B-mode's. Secondly, there are additional sources of B modes such as gravitational lensing of E modes. The latter

[2] specific linear combinations of Q and U insensitive to coordinate rotations

[3] More specifically, when discussing the power spectrum, we will refer to E-mode and B-mode. However, when working with maps, we are going to use Q and U parameters

occurs when light is deflected by massive celestial bodies. Therefore, gravitational lensing of the CMB can change the polarization pattern from E-mode to B-mode and also from B-mode to E-mode. However, this latter conversion does not affect E-mode that much as B-mode amplitude is lower than E-mode.

2.2 Representation of CMB maps and power spectrum: Healpix

To study CMB anisotropies, I used different libraries, such as Healpix, a library that allows the manipulation of data on a spherical map. It can be used with both Python and Julia. Maps are divided into several pieces called pixels. The number of pixels is directly linked to the resolution of the maps. Most of the time, we first define the resolution *nside*, which is usually a power of 2, for instance $nside = 512$. Each pixels have its own value, represented by a numpy array, and its own position defined by the Healpix pixelization schemes. The scheme I used is called "Ring", it describes rotations around the North-South axis from the top to the bottom of the sphere. For example, if we assign each pixels its position number, we can see on the map that the top is at 0 while the bottom has the highest value according to the number of pixel -and therefore, the resolution (figure 7)

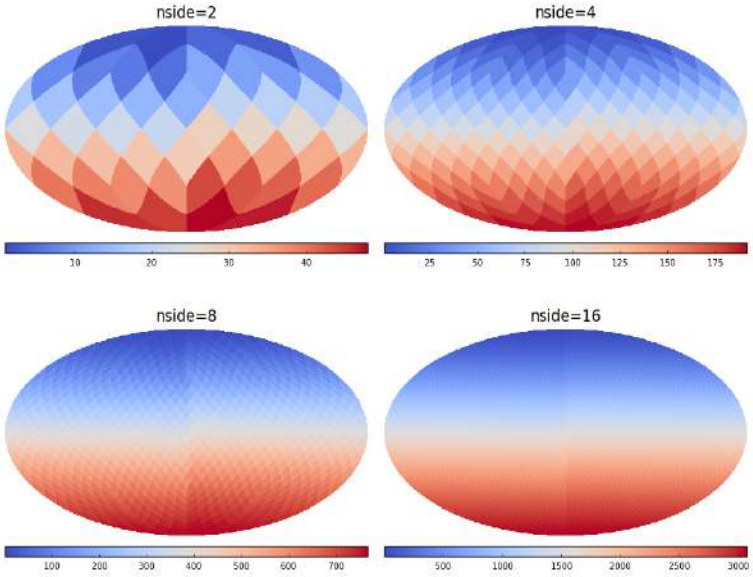

Figure 7: Ring Order, visualization of the scheme for nside=2, nside=4, nside=8, nside=16

Healpix provides many functions. For example, it permits to read maps in the "fits" file format, write maps based on well-structured matrices and display maps with "hp.mollview" function. For instance, below you can see three maps of CMB anisotropies. In figure 8, maps were read from a fits file which contained CMB data - temperature and polarization Q and U.

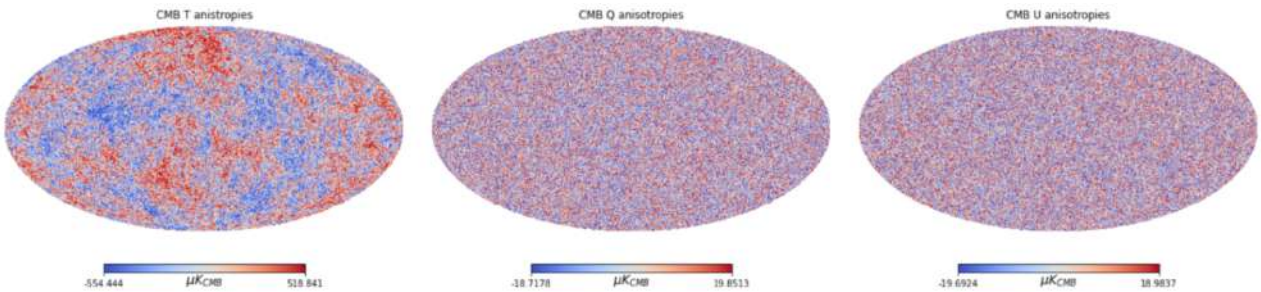

Figure 8: CMB anistropies

As we can see, temperature anisotropies vary on the scale of hundreds of microkelvins while polarization varies on the range of tens of microkelvins. This data can come from previous CMB surveys, such as the Planck mission, or from map making algorithms created to simulate sky maps with CMB components. These latter algorithms typically use the Monte Carlo method.

After observing these maps, we use the hp.anafast function, use to convert a map into a power spectrum. We usually plot all the components in the same figure to make the comparison easier. For instance, figure 9 shows the power spectrum of the previous CMB maps.

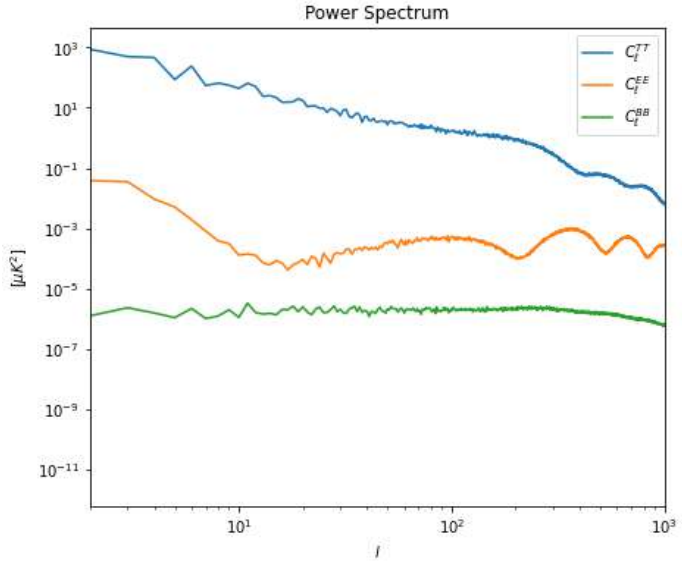

Figure 9: CMB power spectrum

As you can see, the temperature component is higher than the polarization ones, especially for low value of l : four orders of magnitude more than mode E and nine orders more than B-mode -indeed, we saw that E-mode amplitude is higher than B mode. Moreover, the temperature component decreases for larger values of l which means that temperature anisotropies are lower for large angular scales. We can also see that the B-mode component is flat. This is because, in this case, we removed the primordial B-mode. Therefore, what we see is only lensing B-mode. In fact, gravitational lensing converts E-modes into B-modes, so B-mode can be seen as a leakage of E-mode. Since the lensing process is random and that it occurs many times, the distribution of B-modes does not show any specific pattern. Therefore, the power spectrum, which represents the variance, does not show any particular fluctuations along the angular scale, so it is flat.

Power spectrum is a useful tool to explain CMB anisotropies. It is also very important for us because Cl^{BB} is proportional to "r" the ratio between scalar and tensorial fluctuations and, basically, if we calculate this ratio, we will be able to validate whether or not the Cosmic Inflation theory is correct. More precisely, it has been set that if we want LiteBIRD to validate cosmic inflation, the calculation of r should be accurate to ten thousandths. Today, many works are conducted in order to provide such precision.

3 LiteBIRD systematics

3.1 LiteBIRD systematics errors

The error $\delta r < 0.001$ set for LiteBIRD has been divided into three equal parts : statistics, margins and systematics. The statistics are easy to calculate because we know their numerical expressions. Then, margins are also taken into account because of random errors that we cannot predict. Finally, systematic errors are caused by a deviation in data values which means that all the values are shifted in the same direction with the same offset. For example, we must zero a voltmeter before doing any measure otherwise the value will be biased. For LiteBIRD measurements, we count approximately a hundred of systematic errors that need to be controlled with an error less than $\Delta r < \frac{\delta r}{3*100}$, including factors such as beam, noise, and pointing (figure 10)

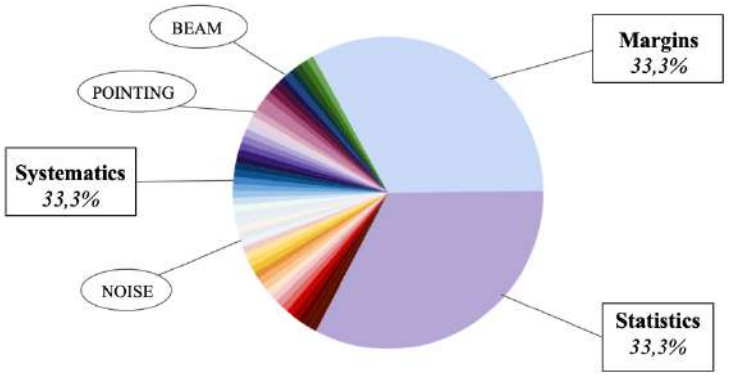

Figure 10: Decomposition of δr between margins, statistics and systematics

For example, beam systematic refers to the error caused by the limited telescope's observation area. To take into account telescopes beam effect, Healpix provides a smoothing function that consists of applying a Gaussian convolution to the Healpix map which averages the values of neighboring pixels. However, the deconvolution operation is not provided by Healpix. During my work, I used a deconvolution function created by Yuya Nagano, a PhD student from the laboratory. This function takes into parameters the alm coefficients, the FWHM and the maximum value of l -Spherical Harmonic parameter- l_{max}. It consists in dividing each group of alm coefficients by another coefficient b_l that depends on the l parameter and the component we are studying -T,Q or U. The function also set to zero every coefficient over $l = 191$ because previous works have shown that the two part we are interesting in are around $l = 4$ and $l = 100$ and, since $nside = 32$ only provides l values unitl $l_{max} = 95$, we choose $nside = 64$ which means $l_{max} = 191$.

Figure 11 shows four CMB temperature maps : the first one is without smoothing, the second is the same map after smoothing operation with a Gaussian with a Full Width at Half Maximum (FWHM) of 5 degrees, the next one is the same map after deconvolution with the same FWHM as before and the last one is the residual temperature CMB beteween the map not smoothed and the deconvolued one.

The residual map shows that the deconvolution operation is not ideal because otherwise the map would be equal to zero. To evaluate the deconvolution function, we prefer to work with the power spectrum. As shown in figure 12, the difference between the not smoothed map we start with (blue curve) and the deconvolved map (green curve) is hardly perceptible until l=191. However, the residual shows a straight increase at l=191 since the deconvolution function has set the alm coefficients to zero (green curve in the bottom). In consequence, the residual curve converges to the not smoothed map (blue curve) which continues to slowly decrease as shown in figure 9. As for the smoothed map (orange curve), the shape is the same as the others for small values of l but it starts to decrease as a quadratic function for higher values since, in power spectrum space, we have the relation $\hat{C}_l = C_l * b_l^2$. You can also see that even though it is smoothed, the component does not completely fallen off, but it describes large fluctuations. This is due to the pixelization effect. In fact, the pixelization of the spherical map cannot represent perfectly the data, it often introduces uncertainties, especially for small angular scales.

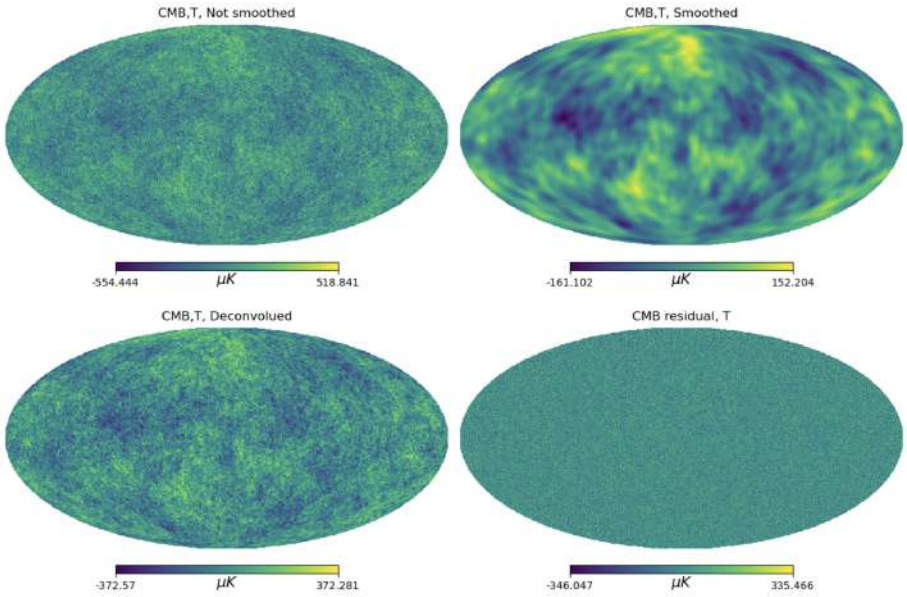

Figure 11: Smoothing operation

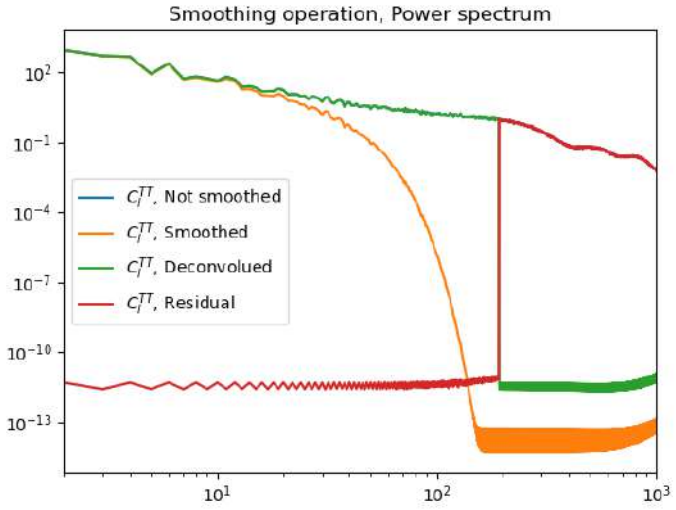

Figure 12: Power spectrum for the smoothing operation

Smoothing operations are really useful for LiteBIRD simulations as telescopes have beams. LiteBIRD satellite aims to detect CMB polarization with the best sensitivity we never had before thanks to "3 telescopes detecting across 15 frequency bands from 34 to 448 GHz with thousands of detectors" (LiteBIRD). In total we count 22 beam sizes (table 1 for LiteBIRD depending on the telescope (LFT,MFT,HFT), the frequency band (15 in total) and the size of the detector (red/yellow VS green/blue ones in LFT as you can see in figure 13).

Therefore, beam effects are not negligible when studying satellite measurements. In the following section, we will present another type of systematics called "pointing systematics". My internship has focused especially on pointing systematics errors but we will continue to include beam effects in the calculations because beam systematics are the one of the most challenging errors.

Telescope	Center Frequency [Hz]	Beam size [arcmin]
LFT	40	70.5
LFT	50	58.5
LFT	60	51.1
LFT	68	(41.6,47.1)
LFT	78	(36.9,43.8)
LFT	89	(33.0,41.5)
LFT/MFT	100	(30.2,37.8)
LFT/MFT	119	(26.3,33.6)
LFT/MFT	140	(23.7,30.8)
MFT	166	28.9
MFT/HFT	195	(28.0,28.6)
HFT	235	24.7
HFT	280	22.5
HFT	337	20.9
HFT	402	17.9

Table 1: LiteBIRD frequency bands and beam sizes

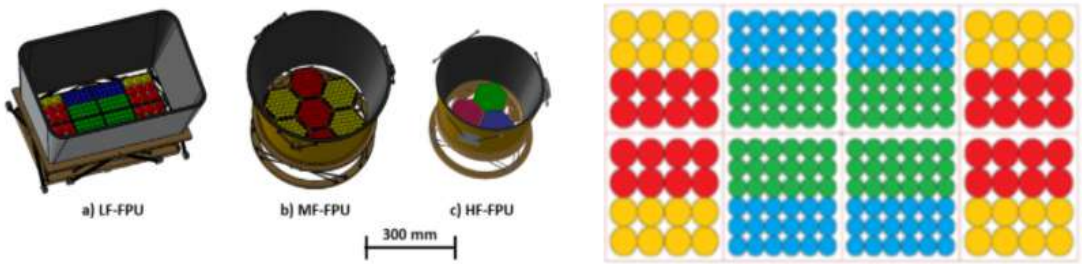

Figure 13: Low, Mid and High-Frequency Telescopes (left) and LFT detectors configuration (right)

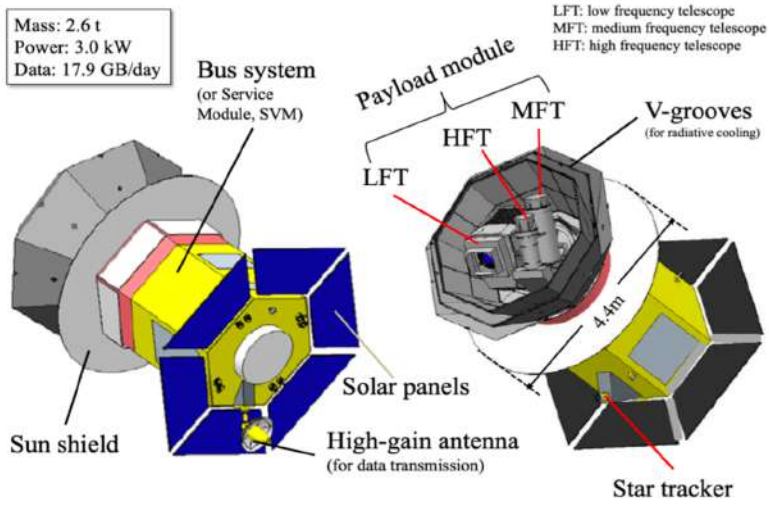

Figure 14: LiteBIRD telescopes

3.2 Introduction to pointing systematics

Pointing systematics are errors that occur when we think we are pointing at a certain point in space when in fact we are slightly off target. These errors are automatically made by the satellite but we can still work to minimize them to a certain threshold. As you can see in figure 15, the pointing

should be at the origin but we are pointing at the red arrowhead. The ρ parameter gives the distance between the two points and χ is the angle between the offset and the scan direction.

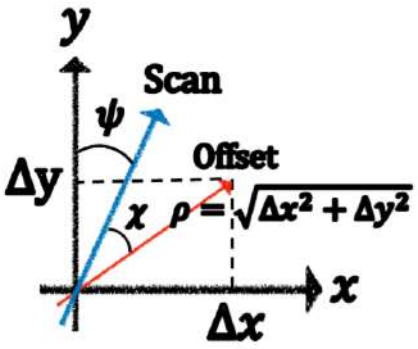

Figure 15: Pointing systematic error

LiteBIRD will contain a star tracker to control this error. Before launching, the angle between the star tracker and the telescope pointing direction, let's say θ_0, will be adjusted to a highly precise value. But, this value is certainly going to change once in space. If we not $\hat{\theta}$ the new angle, we obtain (5).

$$\hat{\theta} = \theta_0 + \theta_b + \sigma_\theta \tag{5}$$

Where θ_b is the bias error and σ_θ is the statistical error. The statistical error σ_b can be eliminate if we repeat the measurements many times (6) :

$$< \hat{\theta} - \theta_0 >= \theta_b \tag{6}$$

The biased error θ_b is also called the "pointing offset". It can be calculated with CMB previous measurements and pointing sources, but the way it will be calculated for LiteBIRD is still under investigation. So, we may wonder **how much pointing offset θ_b is allowed to keep $\delta r < 0.001$?**. To answer at this question, I had to calculate Δr as a function of the pointing offset in order to establish a suitable threshold for the pointing error. To do so, I used a program which permits to calculate reconstructed maps which take into account the pointing errors based on satellite measurements and the scanning strategy of LiteBIRD.

3.3 Reconstructed maps including pointing errors

In order to reconstruct CMB maps including the pointing systematics errors, I used the FALCONS library created by Yusuke Tasake, a PhD student from the laboratory where I worked. FALCONS provides the calculation of pointing TOD (Time Ordering Data) of LiteBIRD knowing the scanning strategy. Besides, the library provides a ScanningStrategy structure, already filled for LiteBIRD.

LiteBIRD will be launched at Lagrange Point 2 ("L2 point"), a point of equilibrium between the Sun and the Earth for low-mass objects thanks to the gravitational influence between the two massive bodies. From this point, LiteBIRD will describe two rotations (figure 16). The first rotation is around the green axis called the "spin axis" with an angle of $\beta = 30°0.1rpm$ and the second rotation is the one of the spin axis around the Sun-Earth direction with an angle of $\alpha = 65°90min$.

Therefore, the Scanning Strategy structure of Falcons requires α and β values but also, the rotation speeds, the sampling rate, the scan duration, the starting point etc. Falcons is already set for the LiteBIRD instrument but of course we can change the values if we need to. For instance, scanning duration of LiteBIRD is three years, but figure 17 shows LiteBIRD's scan path during 5000s, 1 day, 1 month and 1 year. We used to call these maps "hitmaps" because they show how often we hit the pixels as we scan.

Once we know the scanning strategy, we are able to create a reconstructed map including the pointing errors, based on satellite measurements. For instance, in figure 18, you can see that on the left we have a temperature map without any offset based on previous measurements and on the right we displayed the reconstructed map with 1 arcmin pointing offset.

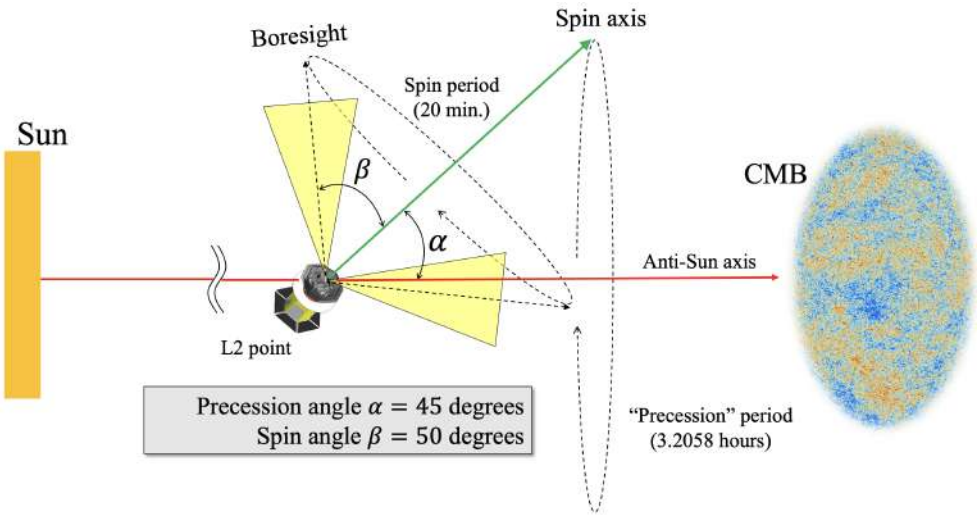

Figure 16: LiteBIRD scanning strategy

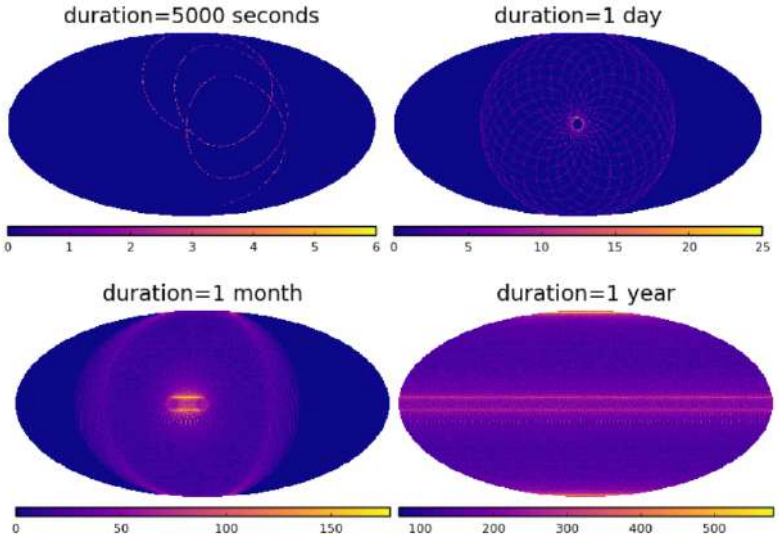

Figure 17: LiteBIRD scanning path for 5000s, 1 day, 1month and 1 year

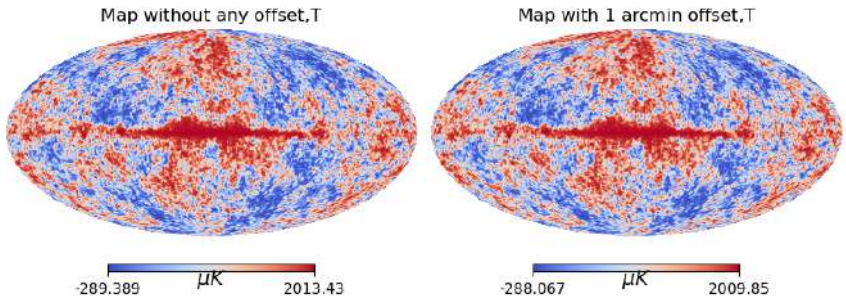

Figure 18: Reconstructed map program results with 1 arcmin offset (temperature)

To conclude, there are many errors that must be controlled in order to determine the ratio r. In this work, we are going to take into account pointing systematics and LiteBIRD beam sizes. We will also consider the additional radiation called "foregrounds" to provide a more accurate CMB analysis.

4 Foregrounds

4.1 Introduction to Foregrounds

In addition to the CMB, LiteBIRD satellite observes many other types of radiation from celestial objects. These are called foreground radiation. One of these is called "Synchrotron" radiation. This latter is caused by the spiral motion of relativistic electrons in the galactic magnetic field. It is a non-thermal radiation but it has a strong linear polarization so it is very important to us. The other foreground we are interested in is dust radiation. In fact, dust absorbs visible and ultraviolet light emitted by stars and re-emits it in the radio and infrared regions. It contains thermal and linear polarization. Figure 19 is extracted from [11], it describes the distribution of these latter foregrounds across the frequencies.

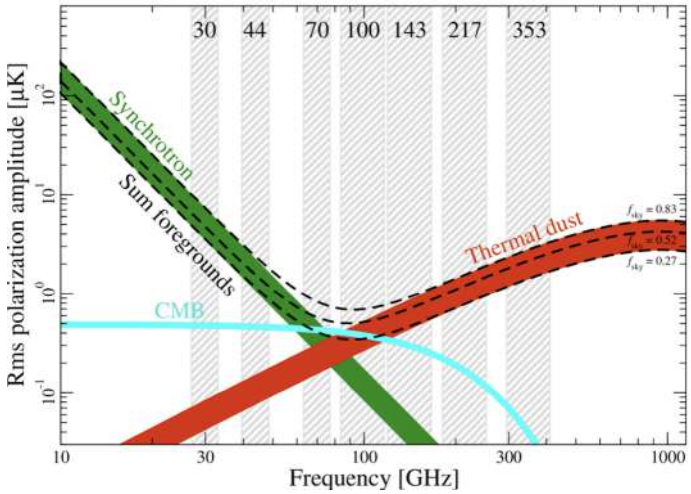

Figure 19: Distribution of Foregrounds across the frequency

Since we want to extract only the CMB polarization from the observed data, we need to remove these foregrounds in an optimal way. In the following, we will focus especially on synchrotron and dust, because they are the main components to remove for CMB analysis, although they are not the only ones. The operation to isolate the signal is called "component separation". It aims, as the name suggests, to separate the different components of the sky -for instance, synchrotron, dust and CMB components. The component separation is based on the distribution of the radiations across the frequency which we got from previous mission like Planck. We can introduce the S/N ratio : the ratio of signal power to noise power (units in decibels [dB]). In this case, the signal refers to the CMB radiation while the noise refers to the dust and the synchrotron.

Foreground radiation has a particularly strong signal in the region of the galactic plane in the sky. The signal-to-noise ratio, S/N, is poor which can introduce large errors due to the uncertain nature of the radiation model. Therefore, a process called "mask" is used to reduce the component separation of the CMB in the galactic plane. We selectively mask regions in the galactic plane where foregrounds dominate in order to minimize their influence on the component separation. This allows us to focus more on the regions of the sky where the CMB signal is more dominant.

4.2 Preparation of Foregrounds and Component separation

FGBuster is the package we use to generate foregrounds and apply the component separation. It needs information about the instrument we are using. The following instruction assigns many details about LiteBIRD to "instrument" such as instrument set up, frequency bands and beam size.

```
instrument=get_instrument("LiteBIRD_IMOvl_full")
```

Then, we use FGBuster to get access to the data, whether it be from observation or simulation. The following instruction assigns to freq-maps a matrix which containing the dust and synchrotron map data -where d0s0 refers is a predefined sky map with dust and synchrotron:

```
freq-maps= get_observation(instrument,"d0s0",nside=512, unit="K_CMB")
```

The dimensions of the resulting matrix are 22 x 3 x 3145728. The value "22" corresponds to the number of maps with different beam sizes. Within these 22 maps, there are 15 different frequency bands. The value "3" refers to the three components of the map -temperature and polarization Q and U- and "3145728" is the data along the pixels according to $nside = 512$. For example, in figure 20 you can see that temperature and polarization maps for the 6th component which means the 6th beam size and the 5th frequency band - 36.9 arcmin beam size and 78.0 GHz frequency band.

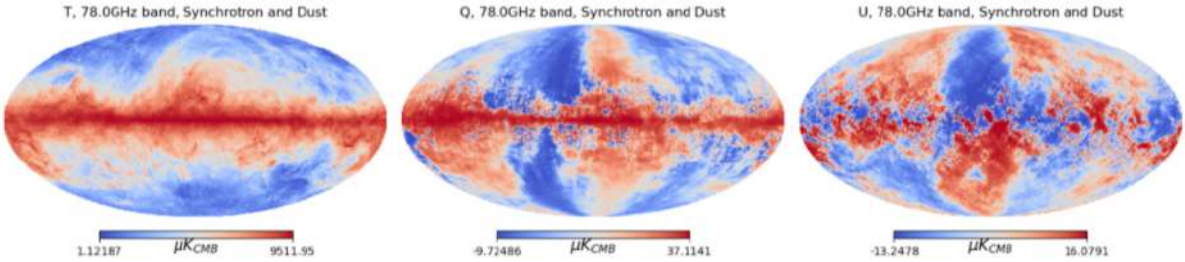

Figure 20: Foregrounds at the frequency $f = 78.0GHz$

Let's add the CMB component given by the predefined CMB data, the results are given figure 21. We can see that the presence of foregrounds is more important for polarization than for temperature which makes the LiteBIRD mission more complicated.

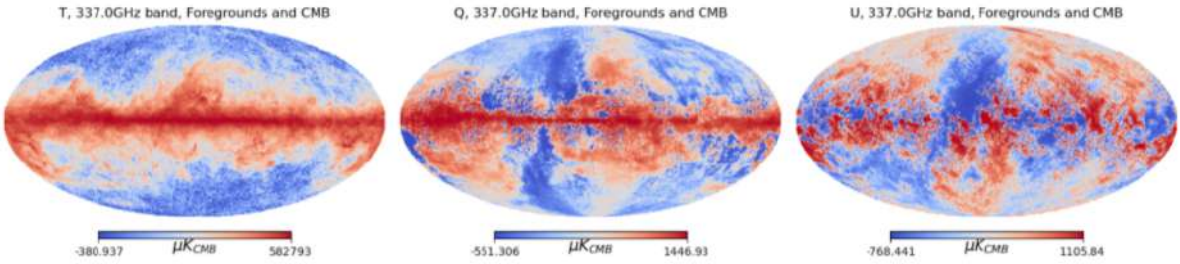

Figure 21: Foregrounds and CMB at the frequency $f = 78.0GHz$

If we remove the CMB from the previous map using the "basic_comp _sep" function and that we study the residual between the CMB extracted and the input CMB we first uploaded, we obtain a map practically equal to zero µK with some errors of the order of $10^{-5}\mu K$ for polarization (figure 22). Therefore, the results of the component separation are acceptable since this function has also its own systematics.

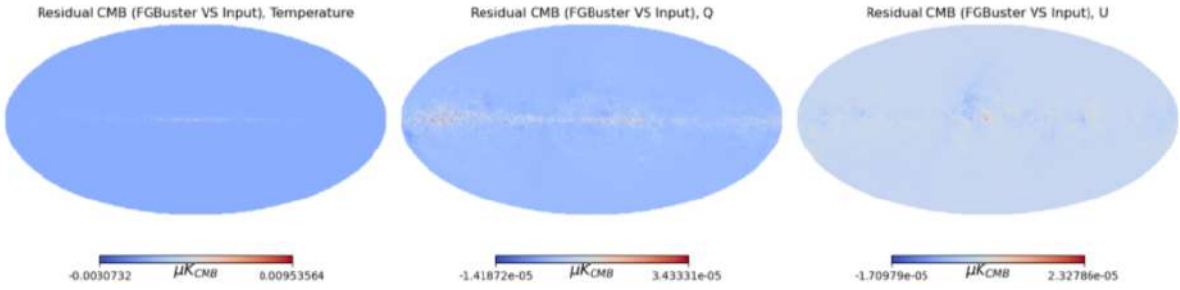

Figure 22: Component separation result. Residual between the input CMB and CMB after the component separation

5 Estimation of Δr

5.1 Resolution scheme

In this section, we are trying to determine a threshold value of the pointing systematic offset in order to provide a precision of $\delta r = 0.001$ which means approximately $\Delta r = \frac{\delta r}{3*100} = 3.3 * 10^{-6}$ for pointing systematic. Therefore, we need to establish a meticulous method in order to take into account both the characteristics of each LiteBIRD telescope and the foregrounds. Below, we present the scheme for a pointing systematic error of 1 arcmin , but further down in this report we will present the results for many other pointing offsets.

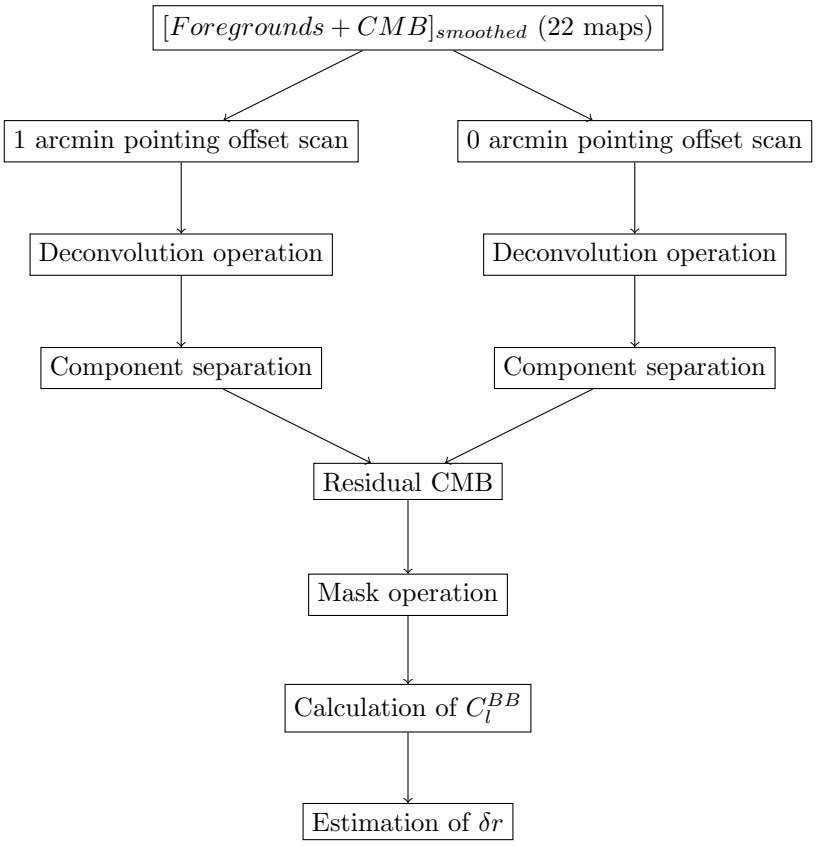

Figure 23: Resolution scheme for the estimation of δr

5.1.1 Generation of Foregrounds and CMB maps

First, we create foreground maps using the FGBuster package. In this case, we will only generate dust and synchrotron because they have the strongest polarization component. We obtain 22 maps, with a resolution $nside = 512$, that need to be smoothed according to the LiteBIRD beam sizes. So, next step is to smooth the 22 maps using the Table 13 while adding the CMB component previously uploaded. Of course, we also smoothed the CMB component with the same beam size as the foregrounds.

Figure 24 shows the T,Q and U maps of foregrounds and CMB smoothed with a beam size equal to 70.5 arcmin before pointing systematics. We note Map 1 because these map corresponds to the ones with the first beam size in Table 13 with the lowest frequency band. As we can see, foregrounds polarization varies on similar scales as CMB ones, roughly on the order of tens of micro kelvins. However, the temperature of foregrounds varies between micro kelvins and thousands of micro kelvins, which is why the temperature scale is larger than before in figure 24.

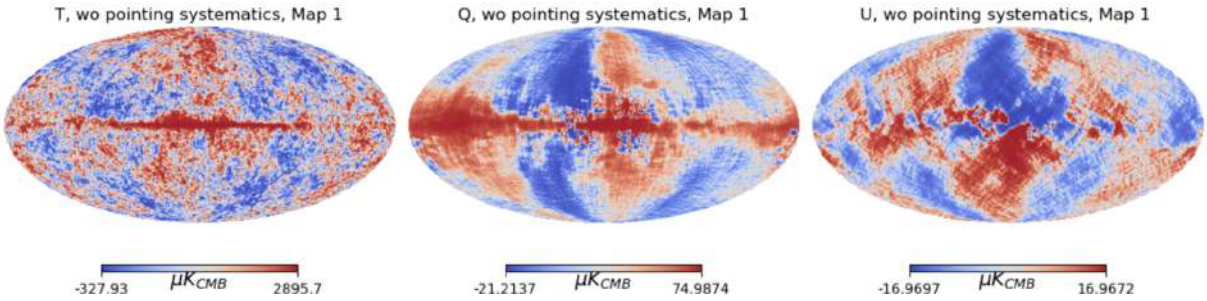

Figure 24: Creation of CMB maps with Foregrounds (dust and synchrotron), smoothed according to the 22 LiteBIRD beam size

5.1.2 Reconstruction of maps with pointing offsets

The next step is to generate the reconstructed maps including the pointing offset. This step has taken a long time to run because we choose a sampling rate of 19 for each map, which means that we made 19 measurements within 1 second during 3 years. We present here the results for 1 arcmin offset. Note that we are also doing the calculations for 0 arcmin even though there should be no difference between the input and output maps since the offset is zero, but it allows us to take into account the error made by the reconstructed map program itself. Figure 25 shows one of the temperature maps [4] for 0 arcmin pointing offset, 1 arcmin and no offset at all and as you can see the difference is very small : on the order of micro kelvin.

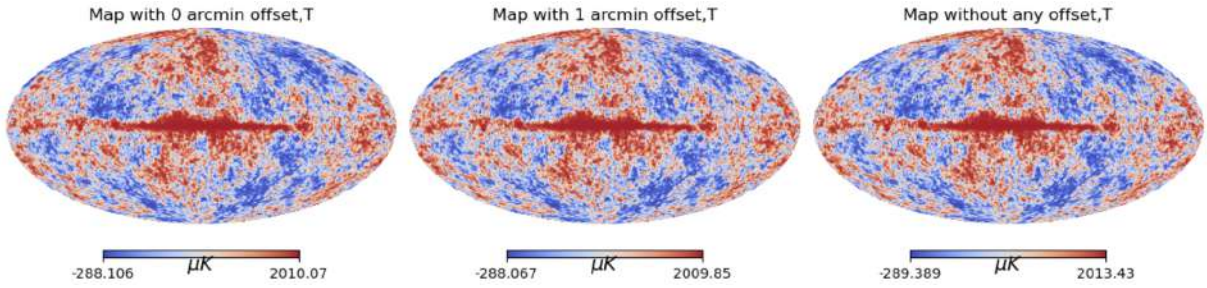

Figure 25: Pointing systematics scan : 0 arcmin offset, 1 arcmin offset, no arcmin offset

5.1.3 Deconvolution

Once we generated the 22 reconstructed maps for each pointing offset, we do the deconvolution operation. In fact, we remove the smoothing effect while applying a deconvolution, using a gaussian function, to each of the 22 maps with their respective beam size coefficients. Figure 26 shows one of the temperature maps before and after the deconvolution operation. As you can see, the map is less smoothed after the deconvolution, we can see more clearly the details of the map.

5.1.4 Component separation and calculation of the residual CMB

After the deconvolution operation, we move on to the component separation. The aim of this latter operation is to extract the CMB component from the 22 maps while removing foreground parts. As for the result, we obtain a $3 * 3 * 3145728$ matrix where the first three dimensions refer to the component we want to extract -CMB, dust or synchrotron-, the next three dimensions is for temperature and polarization -Q and U- and then the 3145728 dimensions contain the data. Figure 27 shows the residual CMB between 1 and 0 arcmin offset. Note that the residual varies on the order of micro kelvins which is quite acceptable considering the errors made along the calculations.

[4] Note that we also did the same thing for polarization maps

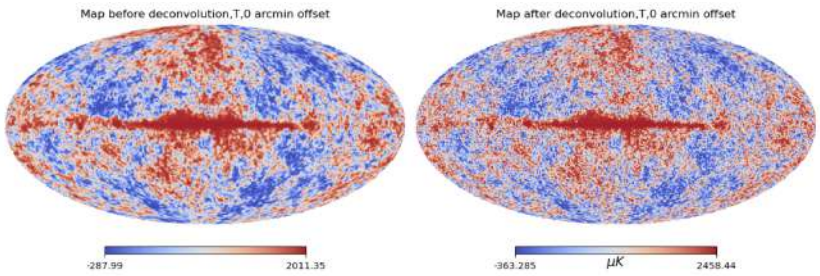

Figure 26: Temperature maps before and after the deconvolution operation

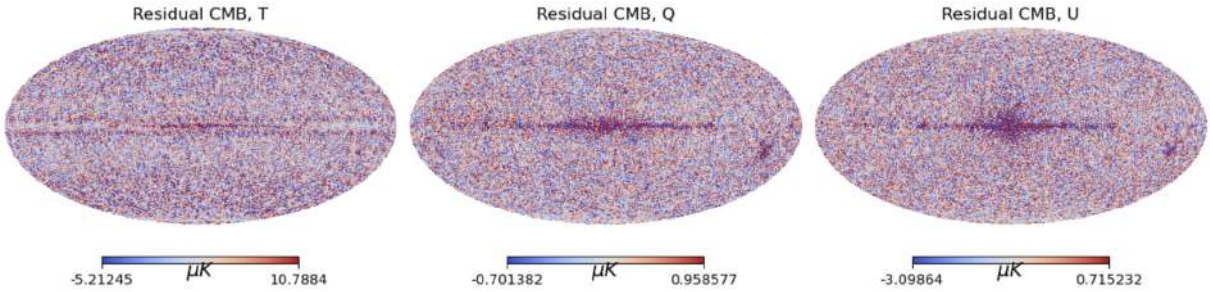

Figure 27: Residual CMB = $CMB_{0arcmin} - CMB_{1arcmin}$

5.1.5 Mask operation

We can continue with these residual maps, but the results are unlikely to be satisfactory because we have missed a phenomenon: foreground radiations are particularly strong in the galactic plane. Therefore, to minimize this effect, we now use a mask, provided by the Planck Legacy Archive. The mask is simply a map set to zero in the galactic plane region and equal to one in the rest of the map[5]. The Planck Legacy Archive is very convenient because it permits to choose the percentage of the map we want to mask. Another particularity is that the frontier between the two regions can be a very distinct line or it can be smoothed. We call this procedure the "apodization". For instance figure 28 shows galactic plane masks, with 40 percent of the map hidden, and two different degrees of apodization. This procedure allows to avoid the ringing artifacts which occur when we transform a signal with a sharp transition into frequency space. In fact, the Fourier transform of a square function is a sinc function. That is why we prefer to convert a signal with a Gaussian shape because the Fourier transform remains a Gaussian function. Therefore, in this work we use a 2 degree apodization.

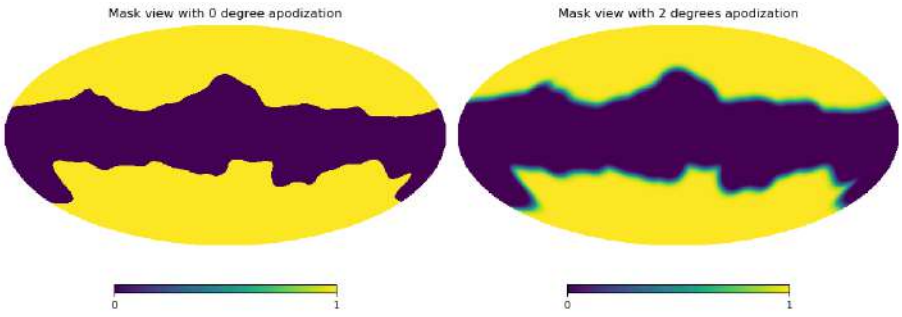

Figure 28: Galactic plane mask with 0 (left) and 2 degrees apodization (right)

Figure 29 shows the residual CMB after applying the mask. As you can see the scale has changed but mostly because the galactic plane contained the largest values in absolute terms. So, when we

[5]So, to apply the mask, we simply have to do a multiplication of the residual map and the mask

remove the galactic plane region, we remove the largest values that is why the scale has been reduced.

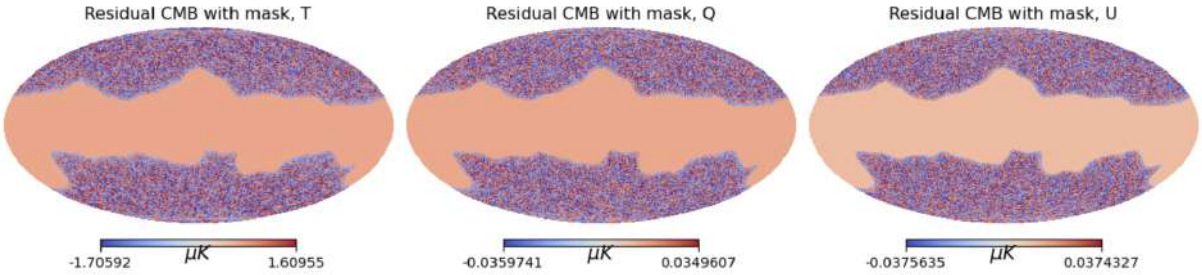

Figure 29: Residual CMB, Temperature and Polarization anistropies with the galactic plane mask

Now that our maps are ready, we can calculate the power spectrum and the Δr value.

5.2 Outcomes

5.2.1 Power spectrum

Figure 30 shows the power spectrum of the residual CMB between 0 and 1 arcmin pointing offset. These figures are obtained with the healpix function $hp.anafast$ which can also permits to differentiate temperature and polarization components, known as E mode and B mode.

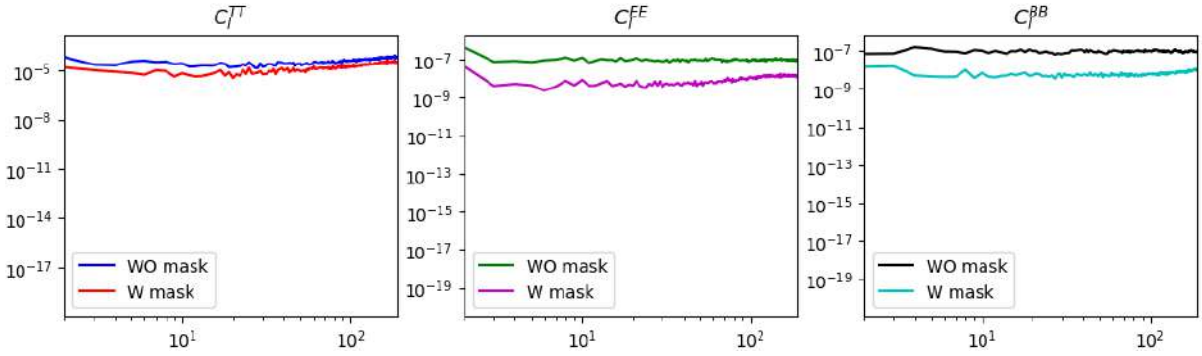

Figure 30: Residual CMB power spectrum (with or without galactic plane mask)

First of all, we see that the mask has reduced the magnitude of the power spectrum. This is mainly due to the reduction of the variation scale when we applied the mask. Secondly, you can see that the temperature component is two orders of magnitude larger than the polarization component which is normal because the power spectrum is a square function of the fluctuation intensity so the previous one-order difference between temperature and polarization components has become two orders with logarithmic function. Then, we can see that the curves of the power spectrum are flat until $l \approx 191$. Actually, when we are looking at the residual CMB, we look at the pointing systematic offset since we have eliminated the CMB component as itself. The offset is constant so there is no reason to have a power spectrum fluctuation across the angular scales. We can also see that when we calculate the power spectrum for different offsets. For instance, figure 31 shows the power spectrum of the residual CMB, with the galactic plane mask, for several pointing offsets.

As you can see, all power spectrum are flat with different magnitudes. The larger the pointing offset is, the larger is the magnitude of the power spectrum. In fact, if we increase the pointing offset, the difference between the data and the zero arcmin pointing offset data also increases so the residual increases. Now that we have the power spectrum, we can determine the Δr as a function of the pointing offset ρ and set a suitable threshold for the poitning offset.

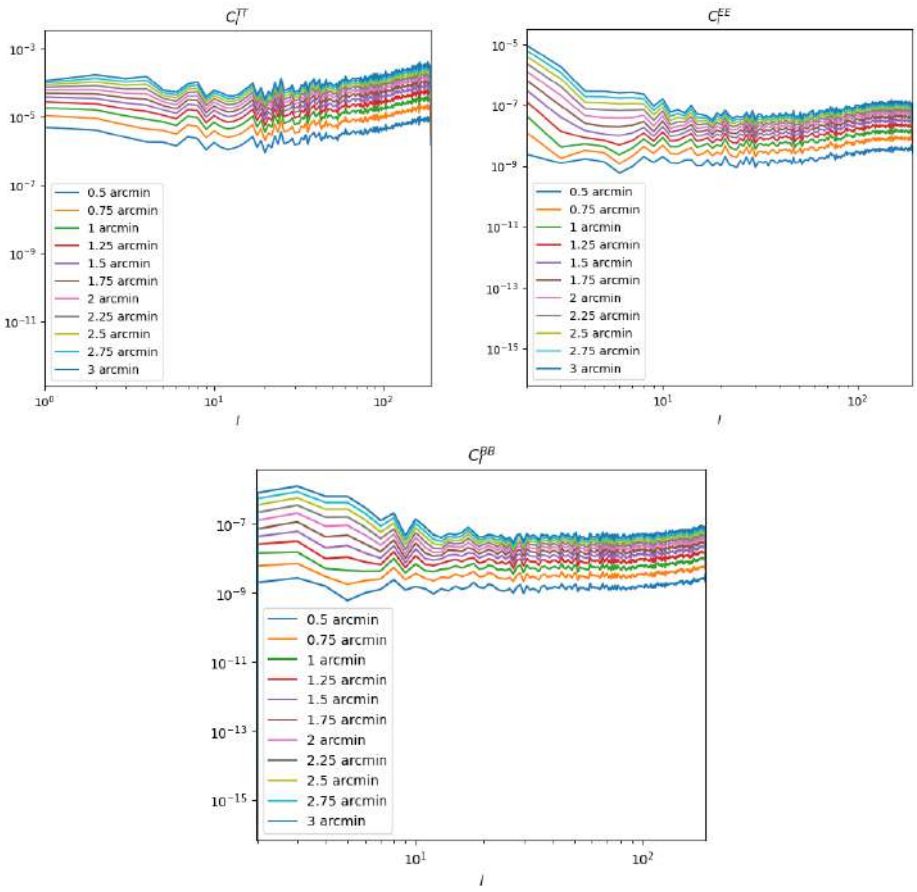

Figure 31: Residual CMB power spectrum for several pointing offsets)

5.2.2 Δr as a function of the pointing systematic offset

To calculate the bias Δr as a function of the pointing offset ρ, I used a predefined function based on "the Formalism of the Errors" in LiteBIRD collaboration (equations detailled in Appendix 1). This function took into parameter the B-mode component of the power spectrum and returns the Δr value as well as the likelihood function whose maximum is Δr.

(Results not given here)

The resulting function has a square behaviour. Let's calculate the Taylor development on a sphere of the polarization between the desired and the truly pointing point (7). This decomposition is possible because the two points are really close in space: let's assume that the desired point is indicated by the vector $\hat{n}$ and that the real pointing point is identified by the vector $\hat{n} + \hat{\rho}$. where $\hat{\rho}$ is the pointing offset.

$$P(\hat{n} + \hat{\rho}) \approx P(\hat{n}) + \left.\frac{\partial P}{\partial r}\right|_{\hat{\mathbf{n}}} \rho + \frac{1}{r}\left.\frac{\partial P}{\partial \theta}\right|_{\hat{\mathbf{n}}} \rho_\theta + \frac{1}{r\sin\theta}\left.\frac{\partial P}{\partial \phi}\right|_{\hat{\mathbf{n}}} \rho_\phi \tag{7}$$

By dimensional analysis, equation (7) gives that the pointing systematic offset is proportional to polarization units (8).

$$\rho \propto P \tag{8}$$

Moreoever, earlier in this report, we assume that Δr is proportional to the B-mode power spectrum C_l^{BB} which units is Kevlin square (9).

$$\Delta r \propto C_l^{BB}[\mu K^2] \propto P^2[\mu K^2] \tag{9}$$

Therefore, if we apply a square operation on equation (8), Δr should be proportional to ρ^2 (10).

$$\Delta r \propto \rho^2 \tag{10}$$

So, it seems that the shape of the curve is quite acceptable even though it is not perfectly square. Nevertheless, this representation is not optimal because it seems difficult to estimate precisely a suitable threshold for Δr. We prefer using a logarithmic scale for Δr as shown in the figure. This figure also shown the threshold $\Delta r = 3.3 * 10^{-6}$ that must not be exceed in order to validate the Cosmic Inflation theory.

(Results not given here)

According to these results, the needed calibration accuracy should be less than (Not given here). This value seems reasonable. However, it is quite small, so it is difficult to implement. We rather expect a value of the order of several arcmin. In the following section we will compare our resolution method with another one, really close, made by a former student of the laboratory.

5.2.3 Comparison to another resolution method

In this section, we compare our results with those we obtained by slightly changing the resolution method. In fact, I used a study of a former student of the laboratory. His method consists of applying an undergrading operation to the maps before the deconvolution and the component separation with the healpix command :

```
MAP_under_graded=hp.ud_grade(MAP,nside_new)
```

In this comparison we under grade the map so that the resolution is no more $nside = 512$ but is now $nside\_new = 64$. We show Δr as a function of ρ for the both method, with or without under grading. We also added the limit $\Delta r < 3.3 * 10^{-6}$ that must not be exceed.

(Results not given here)

You can see that with the points we calculated, the estimation of the threshold is the same: (Not given here). However, we can see that this slightly change resulted in to two very distinct curves. Furthermore, the power spectrum are not the same. For example, in the figure, we display the difference between the power spectrum for 1,2 and 3 arcmin pointing offsets.

You can see that, the more we increase the pointing offset, the more we see a difference for low values of l: the undergrading curve shows a bump while no undergrading curve does not. We believe this effect is due to the fact that, even though the resolution is better without undergrading, the statistics are better with undergrading operation because it averages the data in the same neighborhood of pixels. That is why we think that we saw the bump in one case and not in the other.
So, the threshold we set is really important for the design of LiteBIRD because it allows to respect the error we set for the estimation of the ratio r. If we do not exceed the threshold $\Delta r = 3.3 * 10^{-6}$, we will be able to validate or not the Cosmic Inflation theory thanks to the LiteBIRD measurements. However, there are still a lot of additional parameters we must take into account in order to estimate an accurate value for ρ. For example, this comparison has shown the importance of statistical effects. We could also have calculated more points around $\Delta r = 3.3 * 10^{-6}$. Another parameter we could have thought about is to the direction of the offset. In fact, during this work, we shifted the pointing offset in the same direction for each of the 22 maps but we could have randomly changed the direction of the offset by changing the value of χ (see figure 15) in the LiteBIRD scanning strategy.

Nevertheless, we can admit that the threshold (Not given here) is an acceptable first estimation of the pointing offset ρ for the purpose of the LiteBIRD project. These results could be useful for eventual comparisons to future estimations of Δr using tools other than Falcons or FGBuster, such as `litebird_sim` (see litebird_sim github) which is currently used by many researchers working on the LiteBIRD project.

Conclusion

My work during this internship was to estimate a threshold for the pointing offset ρ of the LiteBIRD instrument to be able to validate or not the theory of cosmic inflation. First, I learned how to use the common tools to manipulate the CMB data in the sky. Then, I familiarized myself with the pointing systematic errors by practicing with the program that allows to reconstruct a map with pointing errors. After that, I started my resolution of the pointing error threshold, taking into account the instrument beams and the foregrounds that need to be removed from the data. This resolution led me to the conclusion that we need a pointing offset of (Not given here) to meet the specification $\Delta r = 3.3 * 10^{-6}$, needed to validate the cosmic inflation theory. This value is small, but it does not seem too unreasonable either since we are looking for an unprecedented precision to explain the very first moments of the universe. However, some technical improvements can be made. For example, a future approach could be to change the direction of the pointing offset between the different telescopes.

Finally, this internship enabled me to make a good progress in computer simulation. It also permits me to learn how to fit into a team and gain in autonomy. But above all, it was a great experience to work in an international environment, whether it was to learn how to communicate in English or to get to know a new culture and a new way to live.

References

[1] *"Introduction to Cosmology" by Barbara Ryden, 2006*
http://carina.fcaglp.unlp.edu.ar/extragalactica/Bibliografia/Ryden_IntroCosmo.pdf

[2] *"The Cosmic Microwave", Science astonishing, 2017*
https://www.youtube.com/watch?v=8WkBP2RU5nw&list=RDCMUCaNlbnghtwlsGF-KzAFThqA&start_radio=1&rv=8WkBP2RU5nw&t=6

[3] *"Modern Cosmology" Second edition, Scott Dodelson and Fabian Schmidt, 2020*

[4] *"Probing Cosmic Inflation with the LiteBIRD Cosmic Microwave Background Polarization Survey", Progress of Theoretical and Experimental Physics, Volume 2023, Issue 4, April 2023, 042F01, Published on November 21th 2022*
https://academic.oup.com/ptep/article/2023/4/042F01/6835420

[5] *"Lensing B-modes in the Cosmic Microwave Background polarization", 2013*
https://astrobites.org/2013/07/24/lensing-b-modes-in-the-cosmic-microwave-background-polarization/

[6] *"From Anisotropies to Polarization", waynehu*
http://background.uchicago.edu/ whu/polar/webversion/node3.html

[7] *"CMB Polarization", 2016*
https://lweb.cfa.harvard.edu/ cbischoff/cmb/

[8] *"LiteBIRD simulation pipeline,Scanning Strategy"*
https://litebird-sim.readthedocs.io/en/lightducc/scanning.html

[9] *"Techniques for Nuclear and Particle Physics Experiments", Second Revised Edition, Springer-Verlag, 1993*

[10] *"Planck Legacy Archive"*
https://pla.esac.esa.int/#home

[11] *"LAMBDA (Legacy Archive for Microwave Background Data Analysis) data products, foregrounds"*
https://lambda.gsfc.nasa.gov/product/foreground/

[12] *"litebird_sim github", Simulation tools for LiteBIRD*
https://github.com/litebird/litebird_sim

[13] *"Empreinte carbone : combien de CO2 émet un Français chaque année ?", Clément Fournier, 2018*
https://ferme.yeswiki.net/Empreinte/?PagePrincipale

[14] *"Recueil de mesures unitaires pour calculer l'empreinte environnementale des activités de recherche"*
https://youmatter.world/fr/emissions-co2-francais-empreinte-carbone/

Résumé

Ce rapport présente le travail que j'ai effectué lors de mon stage dans le laboratoire de cosmologie à l'université d'Okayama. Il traite de l'inflation cosmique, une théorie qui s'insère dans celle du Big Bang et selon laquelle l'univers se serait expandu exponentiellement pendant une période très courte, aux tous premiers instants de l'univers. Cependant, cette théorie reste encore à être prouver. Pour cela, il nous faut étudier les anisotropies de polarisation du fond diffus cosmologique (aussi appelé "rayonnement fossile"), un rayonnement micrométrique qui remplit tout l'espace dans lequel nous vivons. En effet, ce rayonnement aurait été émis par le plasma primordial et présente aujourd'hui des fluctuations de température et de polarisation. Ces fluctuations auraient été créées par les ondes gravitationnelles primordiales émises lors de l'inflation cosmique.

Dans ce rapport, j'explique comment les scientifiques procèdent pour étudier les anisotropies du fond diffus cosmologique. Puis, je présente le projet LiteBIRD qui vise à envoyer d'ici 2030 un satellite pour mesurer les anisotropies de polarisation du rayonnement fossile. Mon travail s'est principalement focalisé sur les erreurs de pointage du satellite. Plus particulièrement, j'ai tenté de déterminer l'erreur de pointage maximale autorisée pour pouvoir valider ou non la théorie de l'inflation cosmique. Ce travail m'a demandé un effort bibliographique très important pour me familiariser au domaine de la cosmologie. Ainsi, par la suite, j'ai pu prendre en compte de nombreux paramètres tels que les erreurs de faisceaux et les rayonnements d'avant-plans qui sont primordiaux pour étudier le fond diffus cosmologique. Finalement, avec ma méthode de résolution et les bibliothèques que j'ai utilisées, j'obtiens un seuil de l'ordre de l'arc minute. Cette valeur semble convenable mais peut encore être affinée, notamment en changeant la direction de l'offset selon les différents télescopes que contient LiteBIRD. Le but étant in fine, de permettre la plus grande erreur de pointage tout en conservant la meilleure précision possible des mesures de polarisation afin de valider la théorie de l'inflation cosmique.

Abstract

This report presents the work I did during my internship at the Laboratory of Cosmology at Okayama University. It deals with cosmic inflation, a theory that is part of the big bang, and according to which the universe expanded exponentially during a very short period of time in the first moments of the universe. However, this theory still need to be proven. To do so, we need to study the polarization anisotropies of the cosmic microwave background (CMB), a microwave radiation that fills all the space in which we live. In fact, this radiation would have been emitted by the primordial plasma and now shows temperature and polarization fluctuations caused by the gravitational waves generated during cosmic inflation.

In this report, I explain how scientists proceed to study CMB anisotropies. Then I present the LiteBIRD project, which aims to launch a satellite around 2030 to measure the polarization anisotropies of the CMB. My work has mainly focused on the pointing errors of the satellite. More specifically, I tried to determine the maximum pointing error allowed to validate or not the cosmic inflation theory. This work required me to make a very important bibliographic effort to familiarize myself with cosmology. This allowed me to take into account many parameters, such as beam errors and foregrounds, which are essential for the study of the CMB. Finally, with my resolution method and the libraries I used, I obtained a threshold of the order of arcminutes. This value seems reasonable, but can be improved by changing the direction of the offset according to the different telescopes included in the LiteBIRD instrument. Finally, the goal was to allow the larger value for the pointing error while keeping the best precision for the polarization measurements in order to validate the cosmic inflation theory.

Appendix 1

This appendix is extracted from "the Formalism of the Errors" in Probing Cosmic Inflation with the LiteBIRD Cosmic Microwave Background Polarization Survey. We describe the link between the B-mode power spectrum C_l^{BB} and Δr.

We define the likelihood function $L(r)$ expressed in the multipole domain :

$$logL(r) = \sum_{l=l_{\min}}^{l_{\max}} logP_l(r) \tag{11}$$

Where $l_{min} = 2$ and $l_{max} = 191$. We also define :

$$\log\ P_l(r) = -f_{sky}\frac{2l+1}{2}\left[\frac{\hat{C}_l}{C_l} + \log\ C_l - \frac{2l-1}{2l+1}\log\ \hat{C}_l\right] \tag{12}$$

Where f_{sky} is a sky map with $f_{sky} = 0.495$. $\hat{C}_l$ is the measured B-mode, we represented it as the following decomposition, assuming there are no primordial B modes (r=0) :

$$\hat{C}_l = C_l^{sys} + C_l^{lens} + N_l \tag{13}$$

Where C_l^{sys} is the estimated systematic effect, C_l^{lens} the lensing B-mode and N_l is the expected noise power spectrum. The modeled power spectrum is:

$$C_l = rC_l^{tens} + C_l^{lens} + N_l \tag{14}$$

Where C_l^{tens} is the tensor mode with r=1. The bias Δr is defined as the value giving the maximum of the likelihood function:

$$\left.\frac{dL}{dr}\right|_{r=\Delta r} = 0 \tag{15}$$

In section 5.2.2, I use a predefined function based on these equations which allowed me to calculate the ratio r from the B-mode power spectrum.